

**OPEN ACCESS**

Repository of the Max Delbrück Center for Molecular Medicine (MDC)  
Berlin (Germany)  
<http://edoc.mdc-berlin.de/3813/>

# Microdomains of GPI-anchored proteins in living cells revealed by crosslinking

---

*Tim Friedrichson and Teymuraz V. Kurzchalia*

Published in final edited form as:

Nature. 1998 Aug 20 ; 394(6695): 802-805 | doi: [10.1038/29570](https://doi.org/10.1038/29570)  
Nature Publishing Group (U.K.) ►

# Microdomains of GPI-anchored proteins in living cells revealed by crosslinking

Tim Friedrichson<sup>1</sup> and Teymuraz V. Kurzchalia<sup>1</sup>

<sup>1</sup> Department of Cell Biology, Max Delbrück Centre for Molecular Medicine, Robert-Rössle-Strasse 10, 13125 Berlin-Buch, Germany

**ABSTRACT** | There is some discussion as to whether glycosyl-phosphatidylinositol(GPI)-anchored proteins occur in microdomains in the cell membrane. These putative microdomains have been implicated in processes such as sorting in polarized cells and signal transduction. Complexes enriched in GPI-anchored proteins, cholesterol and glycosphingolipids have been isolated from cell membranes by using non-ionic detergents: these complexes were thought to represent a clustered arrangement of GPI-anchored proteins. However, results obtained when clustering of GPI-anchored proteins induced by antibodies or by detergents was prevented support the idea of a dispersed surface distribution of GPI-anchored proteins at steady state. Here we use chemical crosslinking to show that membrane microdomains of a GPI-anchored protein exist at the surface in living cells. This clustering is specific for the GPI-anchored form, as two transmembrane forms bearing the same ectodomain do not form oligomers. Depletion of membrane cholesterol causes the clustering of GPI-anchored proteins to break up, whereas treatment of cells with detergent substantially increases the size of the complexes. We find that in living cells these GPI-anchored proteins reside in microdomains consisting of at least 15 molecules, which are much smaller than those seen after detergent extraction.

To study the association of GPI-anchored proteins on the cell surface of intact cells, we used growth hormone (GH) with the GPI-anchoring signal from decay-accelerating factor (DAF) attached to its carboxy terminus (GH-DAF) (Fig.1a). This molecule is an established model for a GPI-anchored protein [14]. When MDCK cells that permanently express GH-DAF (MDCK GH-DAF) were chemically crosslinked at 4 °C with the membrane-impermeable agent bis(sulphosuccinimidyl)suberate (BS3), a prominent band corresponding to a relative molecular mass of 46K (dimer), and a smear from ≈60K to ≈300K were detected, suggesting the existence of microdomains. The crosslinking efficiency for 0.5 mM BS3 was 71%. When crosslinked at 37 °C, the pattern was similar (crosslinking efficiency was 86%), indicating that microdomains also exist at physiological temperatures. Increasing concentrations of BS3 (4 °C) or increasing the incubation time with crosslinker (37 °C) shifted the pattern of crosslinked products to high-molecular-mass forms (Fig.1b). To analyse the oligomers formed, we used the cleavable BS3 analogue 3,3'-dithiobis(sulphosuccinimidyl)propionate (DTSSP) and two-dimensional (2D) electrophoresis. Electrophoresis in the first dimension gave a crosslinking pattern similar to that obtained with BS3, whereas the second dimension under reducing conditions revealed that the crosslinked oligomers consisted primarily of GH-DAF (arrow in Fig.1c); some minor interaction partners were also detected (arrowheads in Fig.1c). Because the length of the spacer arm of BS3 is only 1.14 nm, the detection of crosslinked GH-DAF oligomers indicates that these molecules are close together on the cell surface at steady state. We estimate that the domains consist of at least 15 GH-DAF molecules, because the largest crosslinked species corresponds to a multimer of 15 GH-DAF species. However, the number of GH-DAF molecules in a cluster cannot be defined precisely with this approach: the number is likely to be an underestimate owing to non-saturated crosslinking.

If GH-DAF molecules are crosslinked just because of their relatively high density in cell membranes, there should be a significant difference in crosslinking efficiency in high- and low-expressing clones; but if GH-DAF is confined to

microdomains, there should be a high local concentration of molecules and the extent of crosslinking efficiencies should be independent of the amount of expression. We therefore isolated MDCK clones expressing different amounts of GH-DAF (clones 10 and 16 express 5- and 20-fold more than clone 3, respectively) and used them for crosslinking (Fig.1d). Quantification of the bands on the blot revealed that the crosslinking efficiency was comparable in all clones (86, 81 and 78% for clones 3, 10 and 16, respectively), irrespective of the amount of GH-DAF expressed (Fig.1d). To compare crosslinking patterns, we used the ratio of high-molecular-mass (top third of crosslinked species) to total crosslinked species. These ratios were 30, 23 and 25% for clones 3, 10 and 16, respectively. For all three clones, crosslinking occurred even when the reaction time was very short (2 or 5 min; data not shown), confirming that the GPI-anchored protein was present in domains with a high local concentration.

To investigate whether clustering is specific for GH-DAF, cell lines bearing a transmembrane form of growth hormone were generated: MDCK GH-FL (growth hormone fused to the transmembrane domain of the FcR2-B2 receptor and the cytosolic domain of the low-density lipoprotein (LDL) receptor; Fig.1a) and MDCK GH-FL3YA (in which three cytosolic tyrosine residues have been mutated to alanine). Cells expressing comparable amounts of protein (MDCK GH-FL and GH-FL3YA cells express 73 and 76% of the amount of protein expressed in GH-DAF cl. 10 cells, respectively) were crosslinked with BS3. In contrast to GH-DAF, the amount of GH-FL and GH-FL3YA monomers remaining after crosslinking was unchanged and no oligomers were formed (Fig.1e); the secretory form of GH would not crosslink under a variety of conditions (Fig.1e, and data not shown). Together, these findings indicate that the propensity of GH-DAF to cluster is due to its GPI anchor and not to its protein moiety. Note that GH-DAF and GH-FL3YA are both expressed apically in polarized MDCK cells (data not shown), indicating that microclustering and apical sorting in epithelial cells may not be connected.

Is the clustered organization at the plasma membrane a

general property of GPI-anchored proteins? When other cells (CHO) that permanently express another GPI-anchored protein (the folate receptor, CHO FR-GPI) were crosslinked with BS3, the pattern of crosslinked products was similar to that obtained with MDCK GH-DAF (dimers, trimers and so on) (Fig.2b).

Although the existence of GPI-anchored protein clusters in the plasma membrane of living cells is unproven [2,15], cholesterol depletion leads to a loss of antibody-induced clustering of GPI-anchored proteins [16], an increase in their detergent solubility [17,18], inhibition of folate uptake [19,20] and of signal transduction by GPI-anchored proteins [21]. To see whether cholesterol depletion affected microclustering of GH-DAF and FR-GPI, we treated MDCK GH-DAF cells with methyl- $\beta$ -cyclodextrin [22] and found that the cellular cholesterol content was reduced to 37% of that of control cells, causing the crosslinking of GH-DAF to be inhibited (Fig.2a) and the efficiency to be reduced to 14%; also, the clustering of FR-GPI in CHO FR-GPI cells was almost abolished after extraction of cholesterol (Fig.2b). Results were the same, irrespective of the cholesterol-depletion protocol. Replenishing cholesterol-depleted MDCK GH-DAF cells with cholesterol increased their cholesterol content to 78% and partly restored crosslinking (crosslinking efficiency increased to 25%; Fig.2a). These results indicate that cholesterol-dependent clustering of GH-DAF is partially reversible and in principle could be modulated in the cell, and that the dependence of the integrity of the GPI-anchored protein cluster on cholesterol seems to be a general phenomenon not confined to particular cell types.

The identification of the lectin-like membrane protein VIP36 in detergent-insoluble complexes [23] and of *N*-glycans as possible sorting signals for secreted proteins in MDCK cells [24] has raised the question of whether carbohydrate moieties are involved in transport and/or sorting of GPI-anchored protein. As the GPI anchor consists of both lipid and carbohydrate, we investigated whether carbohydrates are needed to maintain oligomers by crosslinking MDCK GH-DAF and CHO FR-GPI cells in the presence of different monosaccharides (glucose, mannose, inositol and *N*-acetylglucosamine), assuming that excess structural carbohydrates from the GPI anchor might interfere with crosslinking. *N*-acetylglucosamine was used instead of glucosamine, which contains a reactive amino group that would prevent crosslinking. In contrast to the results from cholesterol-depletion experiments, we detected no changes in the pattern of crosslinked products (data not shown).

When the cell membrane is extracted with non-ionic detergents, a fraction enriched in cholesterol, glycosphingolipids and GPI-anchored proteins can be isolated [1,4,10], forming a basis for arguments for the existence of rafts [1]. Others, however, claim that GPI-anchored proteins aggregate only after addition of detergents or antibodies [12,13,15,25]. We investigated the connection between our crosslinked oligomers and the clusters found after detergent extraction of cells by crosslinking MDCK GH-DAF cells after extraction with Triton-X-114 detergent using mild or harsh conditions (see Methods; the latter is commonly used for preparing detergent-insoluble complexes). Mild TX-114 extraction leads to a shift to high-molecular-weight crosslinked products (Fig.3a); this shift is more evident in samples subjected to harsh TX-114 extraction: complexes are so large that only a small fraction (10%) can enter the gel

(Fig.3b, top). Upon cleavage of the crosslinker DTSSP with a reducing agent, 95% of the material is recovered (Fig.3b, bottom). These results indicate that the crosslinked clusters of GH-DAF are significantly smaller than the clusters induced by Triton X-114 treatment: this could be due to the merging of small microdomains [4].

According to the hypothesis of Simons and Ikonen [1], glycosphingolipids and cholesterol can form platforms (rafts) with which some proteins, such as GPI-anchored proteins, are closely associated and from which other membrane proteins are excluded; however, the existence of rafts in living cells, particularly of any containing GPI-anchored proteins, has not been demonstrated. Clustering of GPI-anchored proteins may have been overestimated or small clusters may have escaped detection because of limitations of the microscopical methods used [12]. The results from a fluorescence resonance energy-transfer technique [26] together with those presented here, to our knowledge provide the first evidence for the existence of rafts *in vivo*: we conclude the GPI-anchored proteins reside in membrane microdomains which need cholesterol to be maintained, and that these proteins become heavily aggregated after detergent extraction. We shall not know the exact size or the protein and lipid composition of the rafts until new methods can be devised to isolate rafts without using detergents. This isolation will be difficult because rafts are probably dynamic structures that are constantly exchanging their components [27]. For instance, the discovery of caveolin-1, a protein of the caveolar coat, in detergent extracts enriched in glycosphingolipids, cholesterol and GPI-anchored proteins has led to the proposed existence of rafts containing caveolin-1 and GPI-anchored proteins [10]. However, there is accumulating evidence that there is no enrichment of GPI-anchored proteins in caveolae [25,28,29]; the same is true for trimeric G proteins, which are also found in a buoyant raft fraction but are neither functionally nor morphologically connected with caveolin [30]. The rules governing the interplay between the inclusion and exclusion of proteins into rafts remain to be defined.

## Methods

### Cloning

PCR cloning techniques were used to replace the stop codon of rat growth hormone with a *Bam* HI site creating pSP64GH $\Delta$ C. The same site was added upstream of the GPI-anchoring signal from DAF and cloned into pSP64GH $\Delta$ C to yield pSP64GH-DAF. Plasmid pCBFL5-50 encodes the FcRII-B2 receptor ecto- and transmembrane domains fused to the LDL-receptor cytosolic domain [31]. In pCBFL5-503YA, the three cytosolic tyrosine residues are mutated to alanine. PCR was used to add *Bam* HI sites upstream of the transmembrane sequences, and fragments were cloned in pSP64GH $\Delta$ C to create pSP64GH-FL and pSP64GH-FL3YA, respectively. All constructs were inserted into the mammalian expression vector pRc/CMV (Invitrogen).

### Cells, cell culture and transfection

MDCK cells were maintained in DMEM supplemented with 10% FCS and antibiotics. CHO FR-GPI cells were maintained in folate-free Hams F-12 medium containing 5% FCS, antibiotics and 100  $\mu$ g ml<sup>-1</sup> hygromycin. For

permanent transfection of MDCK cells, the calcium phosphate precipitation method was used.

#### *Crosslinking, electrophoresis and western blotting*

Cells were washed twice with ice-cold PBS and chilled on ice. BS3 or DTSSP were diluted from 25 mM stocks to 0.5 mM with PBS unless indicated otherwise. Except where noted, crosslinking was quenched after 45 min by addition of 50 mM glycine for 15 min. All incubations were at 4 °C. MDCK GH-DAF cells (clone 16, except where noted) were washed with PBS and lysed for 20 min at 4 °C and 10 min at 37 °C in TX-114 lysis buffer (150 mM NaCl; 10 mM Tris-HCl, pH 8.0; 1 mM EDTA; 1% Triton X-114, and protease inhibitors). Lysates were collected, chilled on ice and cleared by 15 min centrifugation at 15,000g. Cleared lysates were subjected to temperature-induced phase separation for 5 min at 37 °C. Aqueous and detergent phases were separated by centrifugation for 3 min at 13,000 r.p.m. at room temperature. To the detergent phases, 0.9 ml Triton X-114 wash buffer (0.06% TX-114, otherwise as TX-114 lysis buffer) was added and vortexed before centrifugation for 15 min at 15,000g (at 4 °C) and another round of phase separation. Detergent phases were precipitated with cold acetone (-20 °C) and boiled for 5 min at 95 °C in Laemmli sample buffer. MDCK GH-FL and GH-FL3YA cells were crosslinked and lysed in TX-114 lysis buffer for 30 min on ice. Cells were scraped and passed three times through a 26-gauge needle to shear the DNA. After 15 min centrifugation at 15,000g at 4 °C, soluble fractions were precipitated with trichloroacetic acid (TCA). MDCK GH cells were incubated for 2 h with PBS containing 0.9 mM Ca<sup>2+</sup> and 0.5 mM Mg<sup>2+</sup> (PBS(+)) and BS3 was added to 0.5 mM directly from a 25 mM stock. Proteins in the supernatant were precipitated with TCA. Pellets were washed with acetone and boiled for 5 min at 95 °C in Laemmli sample buffer. Samples were resolved on 5–15% SDS–PAGE, transferred to nitrocellulose and detected with polyclonal antibodies against GH or folate receptor, HRP-labelled secondary antibodies and ECL. For 2D PAGE, MDCK GH-DAF cells were labelled for 12 h with 80 µCi <sup>35</sup>S-methionine (NEN) and crosslinked with DTSSP. The precipitated detergent phase was boiled in non-reducing sample buffer and resolved on 5–15% SDS–PAGE (1D). The lane was cut and boiled in sample buffer containing 5% β-mercaptoethanol for 5 min at 95 °C and then run on a 5–15% gel (2D) and autoradiographed.

#### *Cholesterol depletion and detergent treatments*

Cells were depleted of membrane cholesterol with 10 mM methyl-β-cyclodextrin in PBS(+) for 1 h at 37 °C. Replenishing with cholesterol was for 6 h at 37 °C with DMEM containing 10% FCS. Cellular cholesterol was measured with an enzyme test kit (Boehringer Mannheim). Protein was determined using a BCA protein assay kit (Pierce). Detergent extractions were done as follows. After washing cells twice with PBS and chilling on ice, samples subjected to mild TX-114 treatment were extracted for 5 min at RT with 0.5% TX-114 in PBS, washed with PBS twice and crosslinked. Harsh TX-114 treatment was done by lysing PBS-washed cells for 30 min at 4 °C in 1 ml TX-114 lysis buffer; cells were scraped and lysates centrifuged for 15 min at 15,000g. The pellets were treated with 950 µl TX-114 lysis buffer and samples were incubated for 10 min at 37 °C, chilled

on ice and crosslinked with BS3 or DTSSP being added directly from 25 mM stocks.

#### *Quantification of western blots*

Quantification of western blots was done with a FUJIX BAS-2000 (Fuji) using <sup>35</sup>S-labelled anti-rabbit IgGs (Amersham) as secondary reagents, or by scanning of low-exposure images after ECL detection using TINA version 2.08 software (Raytest Isotopenmessgeräte GmbH). Crosslinking efficiency for blots incubated with <sup>35</sup>S-labelled IgG was calculated after background subtraction with the formula: (total p.s.l. - p.s.l. of monomer)/(total p.s.l.), where p.s.l. is a measure of the radiation dose that is proportional to d.p.m. For scanned images, optical density was the unit of measurement.

### Acknowledgements

We thank G. Lewin, M. S. Bhojani and M. Wiedmann for critically reading the manuscript; W. Hunziker for plasmids pCBFL5-50 and pCBFL5-503YA; and A. Henske for technical assistance.

### Sources of Funding

This work was supported by the Deutsche Forschungsgemeinschaft and Human Frontier Science Program.

### Corresponding Author

Teymuras V. Kurzchalia; Department of Cell Biology, Max Delbrück Centre for Molecular Medicine, Robert-Rössle-Strasse 10, 13125 Berlin-Buch, Germany; E-mail: kurzchal@orion.rz.mdc-berlin.de

### References

1. Simons, K. & Ikonen, E. Functional rafts in cell membranes. *Nature* 387, 569–572 (1997).
2. Weimbs, T. , Low, S. H. , Chapin, S. J. & Mostov, K. E. Apical targeting in polarized epithelial cells: there's more afloat than rafts. *Trends Cell Biol.* 7, 393–399 (1997).
3. Lisanti, M. P. , Le Bivic, A. , Sargiacomo, M. & Rodriguez Boulan, E. Steady-state distribution and biogenesis of endogenous Madin–Darby canine kidney glycoproteins: evidence for intracellular sorting and polarized cell surface delivery. *J. Cell Biol.* 109, 2117–2127 (1989).
4. Brown, D. A. & Rose, J. K. Dorting of GPI-anchored proteins to glycolipid-enriched membrane subdomains during transport to the apical cell surface. *Cell* 68, 533–544 (1992).
5. Kurzchalia, T. V. *et al.* VIP21, a 21-kD membrane protein is an integral component of *trans* -Golgi-network-derived transport vesicles. *J. Cell Biol.* 118, 1003–1014 (1992).
6. Stefanova, I. , Horejsi, V. , Ansotegui, I. J. , Knapp, W. & Stockinger, H. GPI-anchored cell-surface molecules complexed to protein tyrosine kinases. *Science* 254, 1016–1019 (1991).
7. Brown, D. The tyrosine kinase connection: how GPI-anchored proteins activate T cells. *Curr. Opin. Immunol.* 5, 349–354 (1993).

8. Rodgers, W. , Crise, B. & Rose, J. K. Signals determining protein tyrosine kinase and glycosyl-phosphatidylinositol-anchored protein targeting to a glycolipid-enriched membrane fraction. *Mol. Cell Biol.* 14, 5384–5391 (1994).
9. Fiedler, K. , Kobayashi, T. , Kurzchalia, T. V. & Simons, K. Glycosphingolipid-enriched, detergent-insoluble complexes in protein sorting in epithelial cells. *Biochemistry* 32, 6365–6373 (1993).
10. Sargiacomo, M. , Sudol, M. , Tang, Z. & Lisanti, M. P. Signal transducing molecules and glycosyl-phosphatidylinositol-linked proteins form a caveolin-rich insoluble complex in MDCK cells. *J. Cell Biol.* 122, 789–807 (1993).
11. Hannan, L. A. , Lisanti, M. P. , Rodriguez Boulan, E. & Edidin, M. Correctly sorted molecules of a GPI-anchored protein are clustered and immobile when they arrive at the apical surface of MDCK cells. *J. Cell Biol.* 120, 353–358 (1993).
12. Mayor, S. , Rothberg, K. G. & Maxfield, F. R. Sequestration of GPI-anchored proteins in caveolae triggered by cross-linking. *Science* 264, 1948–1951 (1994).
13. Mayor, S. & Maxfield, F. R. Insolubility and redistribution of GPI-anchored proteins at the cell surface after detergent treatment. *Mol. Biol. Cell* 6, 929–944 (1995).
14. Lisanti, M. P. , Caras, I. W. , Davitz, M. A. & Rodriguez Boulan, E. Aglycophospholipid membrane anchor acts as an apical targeting signal in polarized epithelial cells. *J. Cell Biol.* 109, 2145–2156 (1989).
15. Kurzchalia, T. , Hartmann, E. & Dupree, P. Guilt by insolubility—Does a protein's detergent insolubility reflect caveolar location? *Trends Cell Biol.* 5, 187–189 (1995).
16. Rothberg, K. G. , Ying, Y. S. , Kamen, B. A. & Anderson, R. G. Cholesterol controls the clustering of the glycopospholipid-anchored membrane receptor for 5-methyltetrahydrofolate. *J. Cell Biol.* 111, 2931–2938 (1990).
17. Cerneus, D. P. , Ueffing, E. , Posthuma, G. , Strous, G. J. & van der Ende, A. Detergent insolubility of alkaline phosphatase during biosynthetic transport and endocytosis. Role of cholesterol. *J. Biol. Chem.* 268, 3150–3155 (1993).
18. Hanada, K. , Nishijima, M. , Akamatsu, Y. & Pagano, R. E. Both sphingolipids and cholesterol participate in the detergent insolubility of alkaline phosphatase, a glycosylphosphatidylinositol-anchored protein, in mammalian membranes. *J. Biol. Chem.* 270, 6254–6260 (1995).
19. Chang, W. J. , Rothberg, K. G. , Kamen, B. A. & Anderson, R. G. Lowering the cholesterol content of MA104 cells inhibits receptor-mediated transport of folate. *J. Cell Biol.* 118, 63–69 (1992).
20. Smart, E. J. , Mineo, C. & Anderson, R. G. Clustered folate receptors deliver 5-methyltetrahydrofolate to cytoplasm of MA104 cells. *J. Cell Biol.* 134, 1169–1177 (1996).
21. Stulnig, T. M. *et al.* Signal transduction via glycosyl phosphatidylinositol-anchored proteins in T cells is inhibited by lowering cellular cholesterol. *J. Biol. Chem.* 272, 19242–19247 (1997).
22. Klein, U. , Gimpl, G. & Fahrenholz, F. Alteration of the myometrial plasma membrane cholesterol content with beta-cyclodextrin modulates the binding affinity of the oxytocin receptor. *Biochemistry* 34, 13784–13793 (1995).
23. Fiedler, K. , Parton, R. G. , Kellner, R. , Etzold, T. & Simons, K. VIP36, a novel component of glycolipid rafts and exocytic carrier vesicles in epithelial cells. *EMBO J.* 13, 1729–1740 (1994).
24. Scheiffele, P. , Peranen, J. & Simons, K. N-glycans as apical sorting signals in epithelial cells. *Nature* 378, 96–98 (1995).
25. Fujimoto, T. GPI-anchored proteins, glycosphingolipids, and sphingomyelin are sequestered to caveolae only after crosslinking. *J. Histochem. Cytochem.* 44, 929–941 (1996).
26. Varma, R. & Mayor, S. GPI-anchored proteins are organized in submicron domains at the cell surface. *Nature* 394, 798–801 (1998).
27. Harder, T. & Simons, K. Caveolae, DIGs, and the dynamics of sphingolipid-cholesterol microdomains. *Curr. Opin. Cell Biol.* 9, 534–542 (1997).
28. Schnitzer, J. E. , McIntosh, D. P. , Dvorak, A. M. , Liu, J. & Oh, P. Separation of caveolae from associated microdomains of GPI-anchored proteins. *Science* 269, 1435–1439 (1995).
29. Wu, M. , Fan, J. , Gunning, W. & Ratnam, M. Clustering of GPI-anchored folate receptor independent of both cross-linking and association with caveolin. *J. Membr. Biol.* 159, 137–147 (1997).
30. Huang, C. *et al.* Organization of G proteins and adenylyl cyclase at the plasma membrane. *Mol. Biol. Cell* 8, 2365–2378 (1997).
31. Matter, K. , Hunziker, W. & Mellman, I. Basolateral sorting of LDL receptor in MDCK cells: the cytoplasmic domain contains two tyrosine-dependent targeting determinants. *Cell* 71, 741–753 (1992).

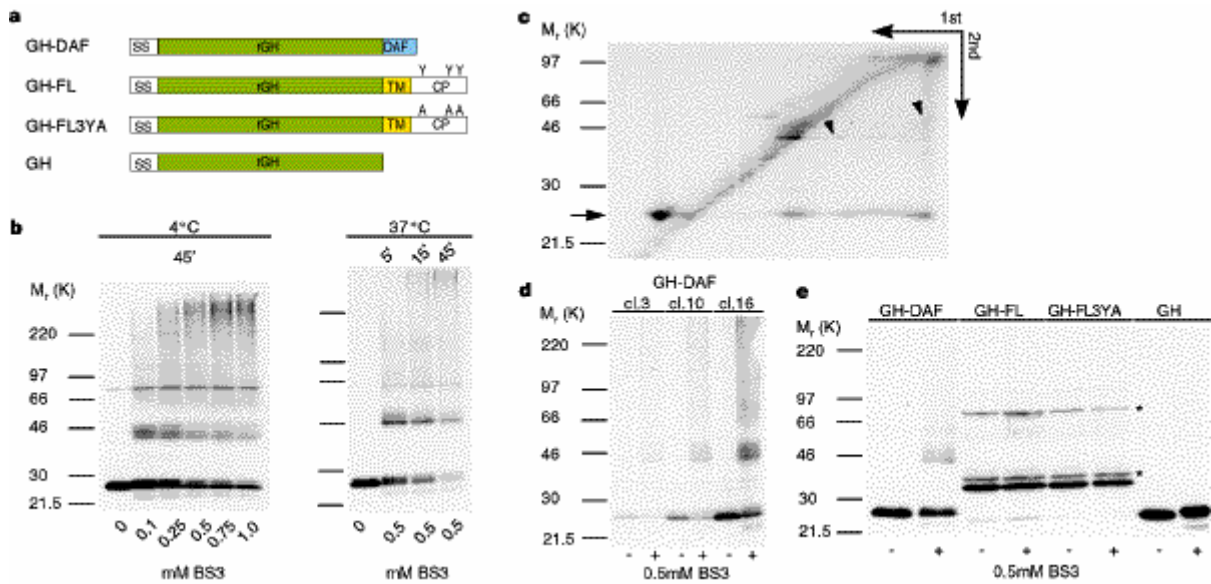


**Figure 1. Detection of oligomers upon crosslinking of GPI-anchored, transmembrane and secretory forms of GH.**

(a) Constructs used for generation of permanently expressing MDCK cells. The GPI-anchoring signal of DAF was fused C-terminally to GH. Transmembrane forms were generated by fusing the FcR11-B2 receptor transmembrane domain and the LDL-receptor cytoplasmic domain to GH. Mutation of the tyrosine residues present in the C-tail to alanine results in apical expression in polarized MDCK cells. (b) Appearance of GH-DAF oligomers induced by chemical crosslinking. MDCK GH-DAF cells were incubated with increasing concentrations of BS3 at 4 °C or for different times with 0.5 mM BS3 at 37 °C. (c) Oligomers formed on crosslinking consist primarily of GH-DAF. MDCK GH-DAF cells were labelled with <sup>35</sup>S-methionine, and after crosslinking were subjected to 2D PAGE. GH-DAF is the principal protein found in the oligomers (arrow). Possible interaction partners are indicated by arrowheads. (d) Crosslinking pattern is independent of the level of GH-DAF expression. Low- (clone 3), medium- (clone 10) or high- (clone 16) expressing clones were used for crosslinking. e, Clustering is a specific property of the GPI-anchored form of GH. MDCK GH-DAF clone 10, GH-FL or GH-FL3YA cells expressing comparable amounts of protein, and MDCK GH cells were crosslinked with BS3. Note that oligomers are detected only for GH-DAF. Asterisk, nonspecific bands obtained upon preparation of TX-114-soluble material (see Methods).

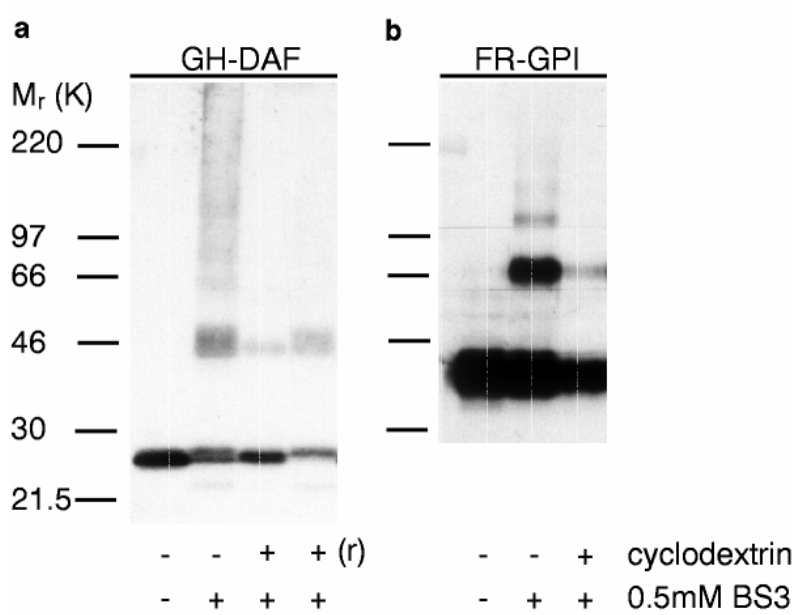


**Figure 2. Clustering of GPI-anchored proteins depends on cholesterol.**

(a), MDCK GH-DAF cells, or (b), CHO FR-GPI cells were treated with 10 mM methyl- $\beta$ -cyclodextrin for 1 h at 37 °C (where indicated) to deplete the membrane of cholesterol. MDCK GH-DAF cells were partially replenished with cholesterol by incubation with DMEM supplemented with 10% FCS for 6 h at 37 °C. After these treatments, cells were crosslinked with BS3.

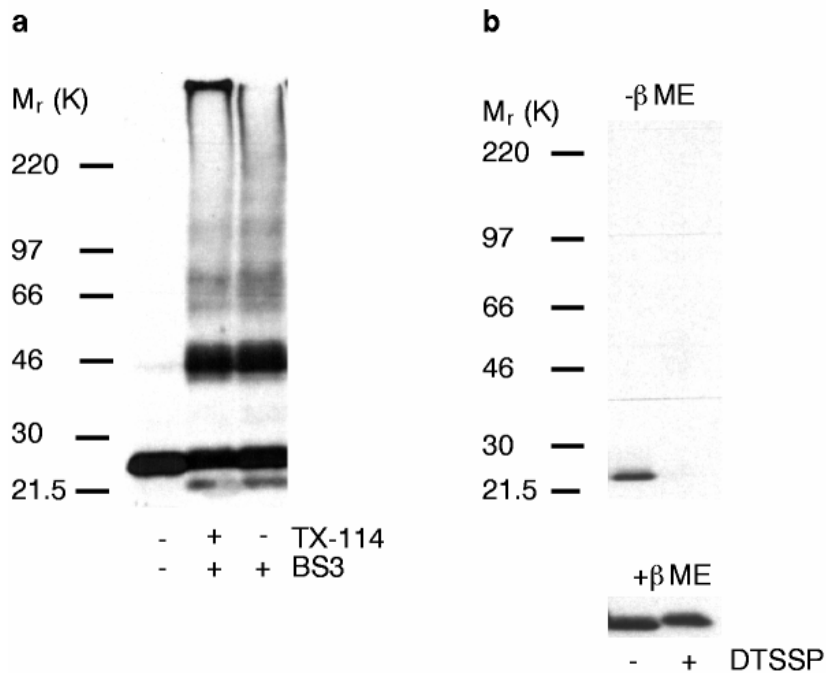


**Figure 3. Detergent treatment leads to increased size of crosslinked oligomers.**

(a) Mild TX-114 extraction shifts the oligomerization pattern of GH-DAF to high-molecular-weight forms. Cells were treated with 0.5% TX-114 for 5 min on ice before crosslinking with BS3. (b) Harsh extraction leads to extreme aggregation of GH-DAF. Cells were extracted for 30 min on ice with 1% TX-114 and the soluble and insoluble fractions separated by centrifugation for 15 min at 15,000g. The insoluble fraction was crosslinked with DTSSP and, after phase separation, the detergent phases were resolved under non-reducing (top) or reducing (bottom) conditions.